Stratospheric Connection to Northern Hemisphere Wintertime Weather: Implications for Prediction

DAVID W. J. THOMPSON

Department of Atmospheric Science, Colorado State University, Fort Collins, Colorado

MARK P. BALDWIN

Northwest Research Associates Inc., Bellevue, Washington

JOHN M. WALLACE

Department of Atmospheric Sciences, University of Washington, Seattle, Washington

(Manuscript received 24 August 2001, in final form 10 December 2001)

ABSTRACT

The dynamical coupling between the stratospheric and tropospheric circulations yields a statistically significant level of potential predictability for extreme cold events throughout much of the Northern Hemisphere (NH) mid–high latitudes on both month-to-month and winter-to-winter timescales. Pronounced weakenings of the NH wintertime stratospheric polar vortex tend to be followed by episodes of anomalously low surface air temperatures and increased frequency of occurrence of extreme cold events throughout densely populated regions such as eastern North America, northern Europe, and eastern Asia that persist for ~2 months. Strengthenings of the vortex tend to be followed by surface temperature anomalies in the opposite sense. During midwinter, the quasi-biennial oscillation (QBO) in the equatorial stratosphere has a similar but somewhat weaker impact on NH weather, presumably through its impact on the strength and stability of the stratospheric polar vortex; that is, the easterly phase of the QBO favors an increased incidence of extreme cold events, and vice versa. The signature of the QBO in NH wintertime temperatures is roughly comparable in amplitude to that observed in relation to the El Niño–Southern Oscillation phenomenon.

1. Introduction

Tropospheric predictability on timescales beyond the 1–2-week limit of deterministic weather prediction is typically viewed as residing in patterns of variability of the coupled ocean–atmosphere system and in the Madden–Julian oscillation. There are recent indications that extended tropospheric predictability may also derive from the dynamical coupling between the stratospheric and tropospheric circulations.

Variability in the circulation of the stratosphere is characterized by timescales considerably longer than those observed in the troposphere. This longer timescale reflects the differing dynamical processes that perturb the circulation about its mean state. Whereas the extratropical tropospheric circulation is continually disturbed by rapidly evolving baroclinic waves, variations in the circulation of the stratosphere are driven largely by relatively slower interactions between the zonal flow and planetary-scale waves dispersing upward from the troposphere.

The most striking example of wave-driven, low-frequency variability in the stratosphere is the equatorial quasi-biennial oscillation (QBO; Reed et al. 1961; Baldwin et al. 2001), a quasiperiodic variation in the direction of the zonal flow in the equatorial stratosphere with a mean period of ~27 months. In Northern Hemisphere (NH) high latitudes, variability of the stratosphere is dominated by the episodic weakening and strengthening of the westerly polar vortex that occurs on timescales of weeks to months during the winter season, in association with vacillation cycles (Holton and Mass 1976; Yoden 1990; Scott and Haynes 1998). The deceleration of the vortex is driven mainly by planetary wave breaking, while the acceleration is driven primarily by relaxation toward radiative equilibrium.

The low-frequency variability that characterizes the circulation of the stratosphere has relevance for weather prediction only to the extent that the circulation of the stratosphere impacts the circulation of the troposphere. This impact could occur directly through the mecha-

Corresponding author address: Dr. David W. Thompson, Dept. of Atmospheric Science, Colorado State University, Foothills Campus, Fort Collins, CO 80523.
E-mail: davet@atmos.colostate.edu

nisms described in Haynes et al. (1991), Hartley et al. (1998), and Black (2002). In this case, anomalous momentum forcing in the extratropical circulation induces a deep, thermally indirect mean meridional circulation below the level of the forcing that acts to transport momentum downward. It is also possible that the circulation of the stratosphere impacts the circulation of the troposphere indirectly through its effect on the refraction of planetary waves dispersing upward from the troposphere. As discussed in Hartmann et al. (2000) and Shindell et al. (2001), anomalous westerly flow in the extratropical stratosphere favors increased equatorward propagation (and hence an anomalous poleward flux of westerly momentum) in the upper troposphere/lower stratosphere, and vice versa.

Anecdotal evidence of the stratosphere's impact on the troposphere can be traced back to Quiroz (1977), who noted that the anticyclonic circulation anomalies associated with the sudden stratospheric warming of January 1977 descended all the way down to the earth's surface. More recently, Baldwin and Dunkerton (1999; 2001, hereafter BD) found that a statistically significant tendency for ''downward propagation'' of extratropical zonal wind anomalies of both signs is evident throughout the historical record. Large amplitude anomalies in the strength of the NH wintertime stratospheric polar vortex frequently precede anomalies of the same sign in the troposphere by 1–2 weeks (Baldwin and Dunkerton 1999), and the tropospheric anomalies tend to persist as long as the anomalies in the intensity of the stratospheric polar vortex, about 60 days (BD). The surface signature of the stratospheric anomalies strongly resembles the surface signature of the NH annular mode (NAM), a planetary-scale pattern of climate variability characterized by an out of phase relationship or seesaw in the strength of the zonal flow along ~55° and 35°N (Namias 1950; Thompson and Wallace 2000), also known as, the Arctic Oscillation (Thompson and Wallace 1998) and the North Atlantic Oscillation (Walker and Bliss 1932; van Loon and Rogers 1978; Hurrell 1995). The high-index polarity of the NAM is characterized by low sea level pressure over the Pole and anomalously strong westerlies along ~55°N. Baldwin and Dunkerton (2001) showed that weakenings of the polar vortex tend to be followed by extended periods in which the NAM is biased toward its low-index polarity (high sea level pressure over the Pole), and vice versa.

Sea level pressure anomalies consistent with the surface signature of the NAM emerge in composites based on the opposing polarities of the QBO in the equatorial stratosphere (Ebdon 1975; Holton and Tan 1980; Baldwin et al. 2001), and time series of the NAM and the QBO exhibit statistically significant coherence on ~27-month timescales (Coughlin and Tung 2001). Presumably, this linkage reflects the impact of the QBO on the intensity and stability of the NH wintertime stratospheric polar vortex (Holton and Tan 1980). Planetary waves originating in the troposphere are more likely to interact with, and hence weaken, the stratospheric polar vortex when the westerly waveguide is confined to the NH extratropics as is the case during the easterly phase of the QBO, than when its extends across the equator into the SH as it does during the westerly phase of the QBO (Holton and Tan 1980). Hence, the easterly phase of the QBO favors a weaker stratospheric polar vortex and—through the linkages observed in BD—anomalies in the tropospheric circulation characteristic of the low-index polarity of the NAM, and vice versa.

Fluctuations in the surface signature of the NAM, in turn, impact the mean temperature and the frequency of occurrence of extreme cold events throughout the NH: low-index conditions are marked by below-normal mean surface air temperatures (Hurrell 1995; Hurrell and van Loon 1997) and an enhanced frequency of occurrence of extreme cold events (Thompson and Wallace 2001) throughout much of North America, Europe, and Asia; high-index conditions are marked by anomalies in the opposite sense.

The observed linkages between low-frequency variability in the stratosphere and the circulation of the troposphere are clearly of theoretical interest, but it remains to be determined to what extent they are of practical use for weather forecasting. Here we gauge their usefulness by assessing the potential predictability of wintertime mean temperatures and the frequency of occurrence of extreme cold events throughout the NH that derives from the influence of the stratospheric circulation upon the surface signature of the NAM. To provide a benchmark for our findings, we compare the results with corresponding statistics pertaining to the El Niño–Southern Oscillation (ENSO) phenomenon.

2. Analysis

This study is based on 42 yr (1958–99) of 4 times daily data from the National Centers for Environmental Prediction–National Center for Atmospheric Research (NCEP–NCAR) reanalysis [Kalnay et al. 1996; obtained from the National Oceanic and Atmospheric Administration (NOAA) Climate Diagnostics Center] supplemented with daily station data over the United States and Japan (obtained from the NOAA National Climate Data Center).

The potential predictability that derives from the downward propagation of long-lived zonal wind anomalies is assessed by comparing the mean daily surface air temperature and the frequency of occurrence of extreme cold events during the 60-day interval following the onset dates of weak and strong vortex conditions in the stratosphere (defined in accordance with the results of BD). Cold events are defined as days on which daily minimum temperature drops more than 1.5 standard deviations (rounded up to the nearest degree Celsius) below the January–February–March (JFM) mean. The on-

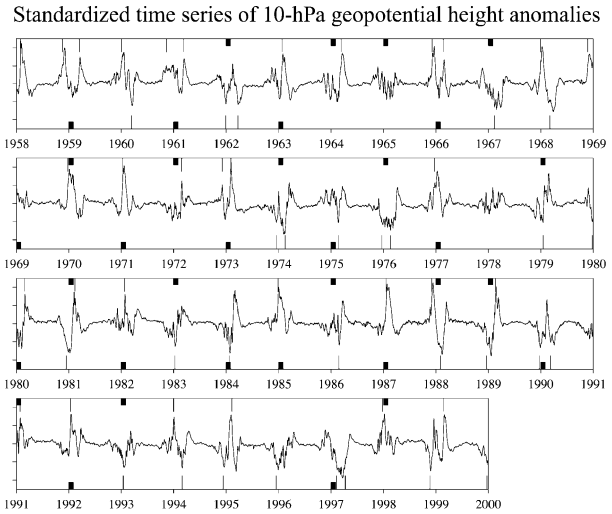

FIG. 1. Standardized daily values of 10-hPa geopotential height anomalies averaged poleward of 60°N. Onset dates for weak and strong vortex conditions are denoted by thin vertical lines at the top and bottom of the figure, respectively; Januarys corresponding to the easterly and westerly phases of the QBO in equatorial winds are denoted by solid boxes at the top and bottom of the figure, respectively (see text for details). Tick marks on the horizontal axis correspond to 1 Jan of the respective years; tick marks on the vertical axis are located at 2 std dev increments.

set dates of weak and strong vortex conditions in the stratosphere are defined as days when daily values of 10-hPa geopotential height poleward of 60°N standardized about the JFM climatology cross the +2 (weak vortex) and −2 (strong vortex) standard deviation thresholds, respectively. The resulting time series (Fig. 1) is dominated by low-frequency vacillations during the NH winter in which anomalies of the same sign typically persist for several weeks, consistent with the discussion in the previous section. Note that the onset dates of weak and strong vortex conditions (denoted by thin vertical lines in Fig. 1) can be defined in real time: they do not depend on how long the stratospheric anomalies persists. If two onset dates occur within 60 days of one another, only the first date is used in the analysis. The analysis is based on all days of the calendar year, but since the thresholds are based on the JFM climatology, all of the extreme cold events and onset dates occur during the winter season. A total of 31 strong onset dates and 28 weak onset dates were used in the analysis, which corresponds to a total sample size of $(31 + 28) \times 60 = 3540$ days.

The potential predictability of NH surface air temperature anomalies that derives from the linkage with the QBO is assessed by repeating the above analysis using, as a basis for the compositing, winters corresponding to the opposing phases of the QBO (as indicated in Fig. 1). Winters corresponding to the easterly phase are defined as those in which the monthly mean 50-hPa zonal-mean zonal winds at the equator in the NCEP–NCAR reanalysis are easterly in all four NH winter months December–March, and vice versa. Winters during which the 50-hPa zonal winds at the equator change sign are unclassified. The analysis is not sensitive to the specific level chosen for defining the phase of the QBO; for example, qualitatively similar results were obtained for QBO indices based on 40-hPa zonal winds from the NCEP–NCAR reanalysis, and for 30-hPa zonal winds based on station data (Marquardt and Naujokat 1997). A total of 17 winters were found to correspond to the easterly and westerly phases of the QBO, respectively (Fig. 1).

TABLE 1. Winters corresponding to warm and cold episodes of the ENSO cycle, as defined as the eight warmest and eight coldest JFM mean sea surface temperature anomalies in the equatorial Pacific cold tongue region (6°S–6°N, 180°–90°W) from 1958 to 1999.

	Years
Warm ENSO winters	1958, 1966, 1973, 1977, 1983, 1987, 1992, 1998
Cold ENSO winters	1968, 1971, 1974, 1976, 1984, 1985, 1989, 1996

The predictability that derives from the ENSO phenomenon is assessed by repeating the analysis that was performed for the QBO, but for composites based on warm versus cold years of the ENSO cycle, as defined by the eight warmest and eight coldest JFM mean sea surface temperature (SST) anomalies in the equatorial Pacific ''cold tongue region'' (6°S–6°N, 180°–90°W). The corresponding JFM mean SST thresholds for the warm and cold phase composites are +0.75 and −0.37 K, respectively. The years included in the warm and cold composites are indicated in Table 1. The SST anomalies that were used as a basis for selecting the years are based on the Comprehensive Ocean–Atmosphere Data Set (COADS; Woodruff et al. 1987).

3. Results

The difference between the surface temperature anomalies averaged over the 60-day period following the onset of weak and strong vortex conditions (Fig. 2, left) are largely consistent with the pattern of surface temperature anomalies associated with the surface signature of the annular mode (Hurrell 1995; Thompson and Wallace 2001): most of the mid–high-latitude landmasses tend to be anomalously cold following the onset of weak stratospheric polar vortex conditions while extreme eastern Canada and North Africa are anomalously warm (the pattern would be entirely consistent with the surface signature of the NAM if eastern Siberia and Alaska were of the opposite sign). Heavily populated regions such as eastern North America, northern Europe, and eastern Asia are ~1–2 K colder following the onset of weak vortex conditions than following the onset of strong vortex conditions. The 60-day interval following the onset of weak vortex conditions is characterized by a higher frequency of occurrence of extreme low tem-

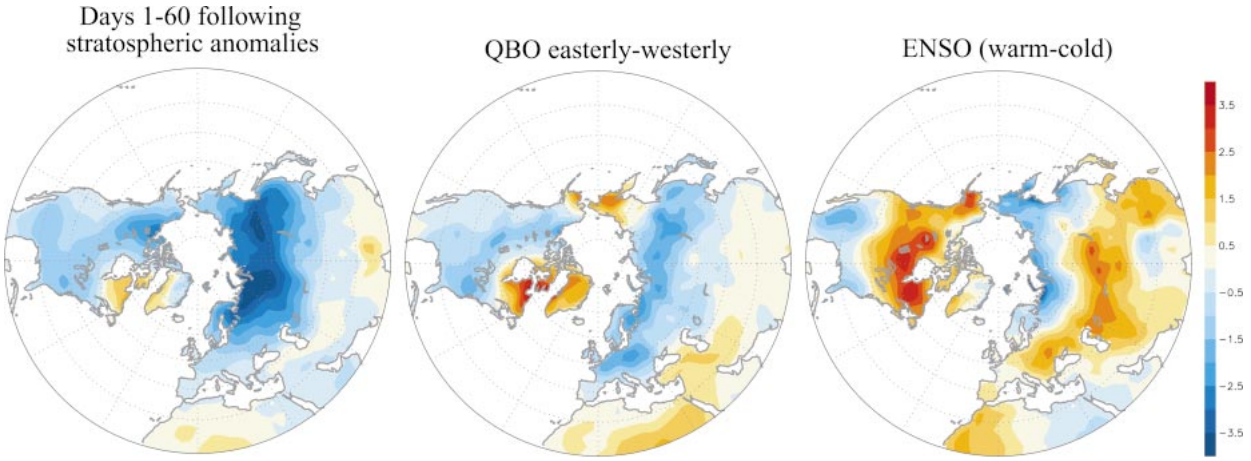

FIG. 2. The difference in daily mean surface temperature anomalies within (left) the 60-day interval following the onset of weak and strong vortex conditions at 10 hPa, (middle) between Januarys when the QBO is easterly and westerly, and (right) between winters (JFM) corresponding to the warm and cold episodes of the ENSO cycle. The samples used in the analysis are documented in Fig. 1. Contour levels are at 0.5°C.

peratures in most large cities that lie in NH midlatitudes, with typical ratios of ~2:1 found across North America to the east of the Rocky Mountains, and throughout northern Europe and Asia (Table 2, columns 3–4).

We define a simple daily index that characterizes the severity of winter temperatures at a given station by relating daily minimum temperature to the JFM climatological mean daily minimum temperature using the relation:

$$\text{wsi}(x, t) = T'^2 \quad \text{for } T' < -\sqrt{2}$$
$$\text{wsi}(x, t) = 0 \quad \text{for } T' \geq -\sqrt{2}$$

where wsi(x, t) are the daily ''winter severity index'' values for station x at time t and T' is the daily minimum temperature standardized about the JFM climatology. The resulting index is affected only by extreme cold events and weights the most extreme ones disproportionately heavily. Since it is calculated relative to the local JFM mean and JFM standard deviation, the wsi exhibits a strong seasonality with peak values in midwinter, and its amplitude does not vary strongly with location. A single index indicative of the severity of winter conditions at major cities throughout the hemisphere [hereafter WSI(t)] can be defined by averaging wsi(x, t) calculated for all the stations listed in Table 2. WSI values composited as a function of calendar date for the 60-day interval following the onset of weak vortex conditions in the stratosphere clearly exceed those for the 60-day interval following the onset of strong vortex conditions throughout much of the NH winter (Fig. 3).

Composites of the WSI for the contrasting phases of the QBO (Fig. 4) exhibit differences consistent with the linkages implied by the discussion in section 1; that is,

TABLE 2. Frequency of occurrence of extreme cold events (days in which daily minimum temperature drops 1.5 std dev below the JFM mean) during the 60-day interval (days +1–60) following the onset of weak and strong vortex conditions at 10 hPa and between Januarys when the QBO is easterly and westerly. The samples are indicated in Fig. 1. Individual results not exceeding the 95% confidence level are italicized.

−1.5 std. temperature threshold	Total	Weak vortex: days +1–60	Strong vortex days +1–60	QBO: easterly	QBO: westerly
<−17°C in Juneau, AK	334	*104*	*66*	96	61
<−18°C in Chicago, IL	411	149	67	115	81
<−6°C in Atlanta, GA	416	149	73	90	56
<−10°C in Washington, DC	392	153	77	96	66
<−9°C in New York, NY	403	164	99	*89*	*69*
<1°C in London, U.K.	442	157	77	85	29
<−3°C in Paris, France	446	148	68	98	48
<−9°C in Stockholm, Sweden	348	154	54	*56*	*23*
<−9°C in Berlin, Germany	450	142	77	107	60
<−22°C in St. Petersburg, Russia	381	137	46	*74*	*46*
<−20°C in Moscow, Russia	472	152	80	*90*	*84*
<−29°C in Novosibirsk, Russia	480	155	69	*67*	*58*
<−4°C in Shanghai, China	471	170	84	*107*	*92*
<−1°C in Tokyo, Japan	328	130	60	92	58

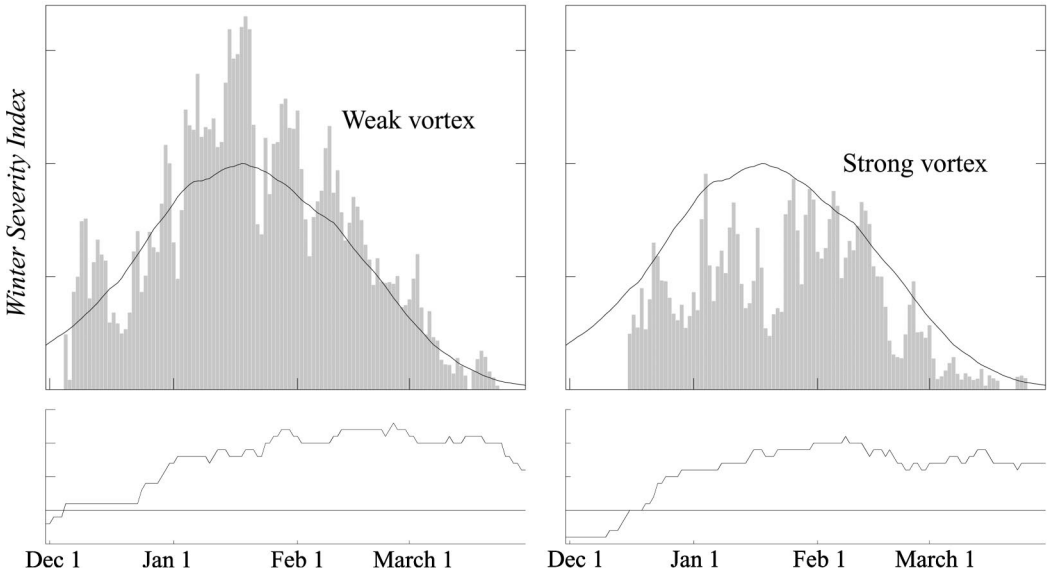

FIG. 3. (top) Daily values of the WSI (as defined in the text) are composited as a function of calendar day for the 60-day interval following the onset of strong and weak vortex conditions at 10 hPa (bars; the climatological WSI is indicated by the parabolic curve). (bottom) The sample size available for each calendar date. Days when the sample size is less than 5 were not included in the composite. Vertical tickmarks are 0.5 for the WSI and 5 for the sample size. The WSI is scaled such that a value of 1 corresponds to the maximum climatological value.

the easterly phase of the QBO favors an increased frequency of occurrence of extreme cold temperatures across the NH midlatitudes, and vice versa. That the largest composite differences in the WSI are found during January (Fig. 4, bottom) is consistent with the facts that the impact of the QBO on the extratropical circulation is largest during early winter (e.g., Baldwin and Dunkerton 1998), and that tropospheric anomalies tend to lag those in the stratosphere by ~2 weeks (Baldwin and Dunkerton 1999; BD). The difference in daily mean temperature between Januarys when the QBO is easterly and westerly (Fig. 2, middle) resembles the signature of the NAM in surface temperature. The mean of the anomalies poleward of 40°N in the middle panel of Fig. 2 (−0.5 K) is ~1/3 of that in the composite derived from the onset of anomalies in the strength of the stratospheric polar vortex (−1.5 K). The corresponding ratios in the frequency of occurrence of extreme cold events at major cities between the contrasting polarities of the QBO (Table 2, columns 5–6) are also weaker than those based on the onset of anomalies in the strength of the stratospheric polar vortex, but they are nevertheless of the expected sign in all cases.

The results in Figs. 2–4 and Table 2 exhibit a high level of statistical significance. The difference in mean temperatures poleward of 40°N (Fig. 2, left), wintertime values of the WSI (Figs. 3–4), and the differences in the frequency of occurrence of extreme events at individual stations in Table 2 can be replicated less than 5% of the time in 10^4 randomized sortings of the data (with the exceptions noted in Table 2). The sortings are generated by randomizing the order of the years in the analysis, but not the days within each calendar year, hence preserving the autocorrelation characteristics of the data. The cumulative significance of the results in Table 2 is even higher: the likelihood that all stations in Table 2 would exhibit differences of the observed amplitude and expected sign by chance is less than 1 in 10^4 for both the 60-day intervals following the onset of weak and strong vortex events and the opposing polarities of the QBO.

4. Comparison with results for ENSO

The results in this section document the impact of ENSO on wintertime mean temperatures and the frequency of occurrence of extreme cold events at select locations over the NH. The results are not meant to constitute a comprehensive review of the impacts of ENSO on NH wintertime weather. They are presented simply to provide a benchmark for the results presented in the previous section.

Figure 2 (right) shows the composite difference in daily mean temperature between winters (January–March) corresponding to warm and cold episodes of the ENSO cycle (as defined in section 2). Consistent with previous results (e.g., Ropelewski and Halpert 1986), the warm phase of the ENSO cycle favors anomalously warm wintertime mean conditions over much of northern North America, and anomalously cold wintertime mean conditions over the southeastern United States. The composites also suggest that warm episodes of the ENSO cycle are characterized by anomalously warm

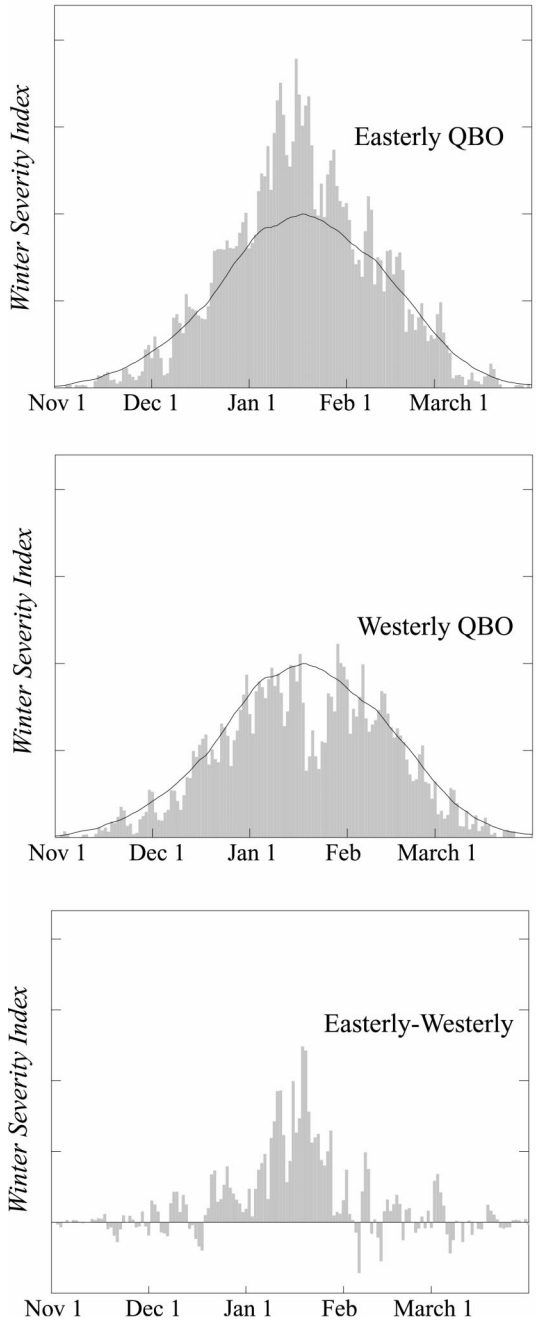

FIG. 4. Daily values of the WSI (bars) for winters when the phase of the QBO is (top) easterly, (middle) westerly, and (bottom) the difference. The climatological WSI is indicated by the solid parabolic line in the top and middle panels. Vertical tick marks are 0.5 for the WSI.

mean temperatures across central Eurasia and cold temperatures over northern Eurasia.

The relative frequencies of occurrence of extreme cold events during the opposing phases of the ENSO cycle are shown in Table 3 for a selection of locations over North America. Winters corresponding to the warm phase of the ENSO cycle are marked by a decreased

TABLE 3. As in Table 2, but for winter seasons (JFM) corresponding to warm and cold episodes of the ENSO cycle (see text for details), and for locations where the impact of ENSO on surface temperatures is relatively strong (e.g., Ropelewski and Halpert 1986).

	Total	Warm	Cold
<-17°C in Juneau, AK	334	32	60
<-24°C in Bozeman, MT	448	26	63
<-4°C in Dallas, TX	416	39	65
<-9°C in Tulsa, OK	464	35	75

incidence of extreme cold events throughout much of northern North America, including regions in the south-central United States where the associated wintertime mean conditions are anomalously cold. The decreased incidence of cold events over the United States during the warm phase of ENSO is consistent with the decreased frequency of occurrence of blocking events over Alaska (Renwick and Wallace 1996), which are associated with cold air outbreaks downstream (Namias 1950). The inverse relationship between the frequency of occurrence of cold events over the south-central United States and the corresponding wintertime mean temperature anomalies exemplifies the importance of assessing the impacts of climate phenomenon on not only the mean climate, but on the frequency of occurrence of extreme events as well. A more thorough treatment of the impact of ENSO on the incidence of extreme cold events is beyond the scope of this paper.

The samples used to assess the impact of the QBO and ENSO on NH wintertime climate have different characteristics: the QBO sample includes 34 winter seasons, but only January days; the ENSO sample includes all days during January–March, but only 16 winter seasons. Additionally, the stations analyzed in the QBO samples are intended to be representative of major cities throughout the NH mid- and high latitudes, whereas those analyzed in the ENSO samples were selected to represent regions in which the impacts of ENSO are known to be strong. Hence, it is difficult to make a direct quantitative comparison between the impact of these two phenomena. Nevertheless, a qualitative comparison of the results based on the QBO and ENSO suggests that for the affected times of year over North America, their impacts are roughly comparable: the differences in the frequency of occurrence of extreme cold events between the easterly and westerly phases of the QBO are similar to those observed during the opposing phases of the ENSO cycle (Tables 2–3), as are the scale and amplitude of the corresponding differences in mean temperature (Fig. 2, middle and right).

5. Concluding remarks

The findings in this study suggest that low-frequency variability in the stratospheric circulation impacts NH wintertime weather on both month-to-month and winter-to-winter timescales. In order to exploit this skill, nu-

merical weather prediction models must have reasonable representations of the relevant stratospheric dynamics. The observed linkage between the QBO and the strength and stability of the NH stratospheric polar vortex has been simulated in numerous modeling studies (e.g., Dameris and Ebel 1990; O'Sullivan and Salby 1990; Holton and Austin 1991; Hamilton 1998; Niwano and Takahashi 1998). As noted in the introduction, this linkage is entirely consistent with northward displacement of the critical latitude for Rossby wave breaking during the easterly phase of the QBO, and vice versa. The observed downward propagation of anomalies in the NH polar vortex has also been simulated in numerical studies (Christiansen 2001). The dynamics of this linkage are still under investigation, but they most likely reflect the impact of anomalies in the strength of the lower-stratospheric polar vortex on the poleward eddy fluxes of zonal momentum in the upper troposphere, and the induced mean meridional circulations that extend all the way down to the earth's surface.

To what extent do the results for days 1–60 following the onset dates of weak and strong conditions in the stratospheric polar vortex reflect predictability beyond the ~10-day limit of deterministic weather prediction? To address this question we restricted the analyses in Table 2 and Figs. 2–3 to days 11–60 following the respective onset dates. In all cases, the significance of the results was unaffected. In several cases, the skill was found to improve slightly (~10%), consistent with the 1–2-week time lag between large amplitude anomalies in the strength of the stratospheric polar vortex and the circulation of the troposphere (Baldwin and Dunkerton 1999). We also tested to what extent recent trends in surface temperatures might bias the results in Tables 2–3 by repeating the analyses with detrended data. Again, in all cases, the significance of the results was unaffected.

We estimated the potential predictability that derives from the downward propagation of zonal wind anomalies using an index indicative of the strength of the NH polar vortex at 10 hPa, which corresponds to the highest level available in the NCEP–NCAR reanalysis. Since vacillation cycles in the stratosphere often originate equatorward of the polar vortex at levels above 10 hPa (e.g., Kodera 1995; Scott and Haynes 1998), it is possible that results based on higher levels will yield an even longer lead time with respect to weather at the surface. Hence, making use of stratospheric data from the Advanced Microwave Sounding Unit (AMSU), it might be possible to make an earlier and more definitive determination of the major swings in the stratospheric polar vortex.

It would be interesting to test the extent to which state-of-the-art numerical models are capable of exploiting both the impact of the QBO on the polar vortex and the downward propagation of stratospheric zonal wind anomalies for making real-time forecasts.

Acknowledgments. We would like to thank R. X. Black and three anonymous reviewers for their helpful comments and suggestions. DWJT was supported by funding provided through Colorado State University and by the National Science Foundation under Grant CA-REER:ATM-0132190; MPB was supported by NOAA Office of Global Programs, the SR&T Program for Geospace Science (NASA), and the National Science Foundation; JMW was supported by the National Science Foundation under Grant 9707069.

REFERENCES

Baldwin, M. P., and T. J. Dunkerton, 1998: Quasi-biennial modulation of the Southern Hemisphere stratospheric polar vortex. *Geophys. Res. Lett.,* **25,** 3343–3346.

——, and ——, 1999: Propagation of the Arctic Oscillation from the stratosphere to the troposphere. *J. Geophys. Res.,* **104,** 30 937–30 946.

——, and ——, 2001: Stratospheric harbingers of anomalous weather regimes. *Science,* **294,** 581–584.

——, and Coauthors, 2001: The Quasi-Biennial Oscillation. *Rev. Geophys.,* **39,** 179–229.

Black, R. X., 2002: Stratospheric forcing of surface climate in the Arctic Oscillation. *J. Climate,* **15,** 268–277.

Christiansen, B., 2001: Downward propagation from the stratosphere to the troposphere: Model and reanalysis. *J. Geophys. Res.,* **106,** 27 307–27 322.

Coughlin, K., and K.-K. Tung, 2001: QBO signal found at the extratropical surface through northern annular modes. *Geophys. Res. Lett.,* **28,** 4563–4566.

Dameris, M., and A. Ebel, 1990: The Quasi-Biennial Oscillation and major stratospheric warmings: A three-dimensional model study. *Ann. Geophys.,* **8,** 79–85.

Ebdon, R. A., 1975: Quasi-biennial oscillation and its association with tropospheric circulation patterns. *Meteor. Mag.,* **104,** 282–297.

Hamilton, K., 1998: Effects of an imposed quasi-biennial oscillation in a comprehensive troposphere–stratosphere–mesosphere general circulation model. *J. Atmos. Sci.,* **55,** 2393–2418.

Hartley, D. E., J. Villarin, R. X. Black, and C. A. Davis, 1998: A new perspective on the dynamical link between the stratosphere and troposphere. *Nature,* **391,** 471–474.

Hartmann, D. L., J. M. Wallace, V. Limpasuvan, D. W. J. Thompson, and J. R. Holton, 2000: Can ozone depletion and greenhouse warming interact to produce rapid climate change? *Proc. Natl. Acad. Sci.,* **97,** 1412–1417.

Haynes, P. H., C. J. Marks, M. E. McIntyre, T. G. Shepherd, and K. P. Shine, 1991: On the ''downward control'' of extratropical diabatic circulations by eddy-induced mean zonal forces. *J. Atmos. Sci.,* **48,** 651–678.

Holton, J. R., and C. Mass, 1976: Stratospheric vacillation cycles. *J. Atmos. Sci.,* **33,** 2218–2225.

——, and H.-C. Tan, 1980: The influence of the equatorial quasi-biennial oscillation on the global circulation at 50 mb. *J. Atmos. Sci.,* **37,** 2200–2208.

——, and J. Austin, 1991: The influence of the QBO on sudden stratospheric warmings. *J. Atmos. Sci.,* **48,** 607–618.

Hurrell, J. W., 1995: Decadal trends in the North Atlantic Oscillation region temperatures and precipitation. *Science,* **269,** 676–679.

——, and H. van Loon, 1997: Decadal variations in climate associated with the North Atlantic Oscillation. *Climatic Change,* **36,** 301–326.

Kalnay, E. M., and Coauthors, 1996: The NCEP/NCAR 40-Year Reanalysis Project. *Bull. Amer. Meteor. Soc.,* **77,** 437–471.

Kodera, K., 1995: On the origin and nature of the interannual variability of the winter stratospheric circulation in the Northern Hemisphere. *J. Geophys. Res.,* **100,** 14 077–14 087.

Marquardt, C., and B. Naujokat, 1997: An update of the equatorial QBO and its variability. *Stratospheric Processes and Their Role in Climate (SPARC): Proc. First SPARC General Assembly,* Vol. 1, Melbourne, Australia, WCRP-99, WMO/TD-814, 87–90.

Namias, J., 1950: The index cycle and its role in the general circulation. *J. Meteor.,* **7,** 130–139.

Niwano, M., and M. Takahashi, 1998: The influence of the equatorial QBO on the Northern Hemisphere winter circulation of a GCM. *J. Meteor. Soc. Japan,* **76,** 453–461.

O'Sullivan, D., and M. L. Salby, 1990: Coupling of the quasi-biennial oscillation and the extratropical circulation in the stratosphere through planetary wave transport. *J. Atmos. Sci.,* **47,** 650–673.

Quiroz, R. S., 1977: Tropospheric-stratospheric polar vortex breakdown of January 1977. *Geophys. Res. Lett.,* **4,** 151–154.

Reed, R. J., W. J. Campbell, L. A. Rasmussen, and R. G. Rogers, 1961: Evidence of downward propagating annual wind reversal in the equatorial stratosphere. *J. Geophys. Res.,* **66,** 813–818.

Renwick, J. A., and J. M. Wallace, 1996: Relationships between north Pacific wintertime blocking, El Niño, and the PNA pattern. *Mon. Wea. Rev.,* **124,** 2071–2076.

Ropelewski, C. F., and M. S. Halpert, 1986: North American precipitation and temperature patterns associated with the El Niño/Southern Oscillation (ENSO). *Mon. Wea. Rev.,* **114,** 2352–2362.

Scott, R. K., and P. H. Haynes, 1998: Internal interannual variability of the extratropical stratospheric circulation: The low-latitude flywheel. *Quart. J. Roy. Meteor. Soc.,* **124,** 2149–2173.

Shindell, D. T., G. A. Schmidt, R. L. Miller, and D. Rind, 2001: Northern Hemisphere winter climate response to greenhouse gas, ozone, solar, and volcanic forcing. *J. Geophys. Res.,* **106,** 7193–7210.

Thompson, D. W. J., and J. M. Wallace, 1998: The Arctic Oscillation signature in the wintertime geopotential height and temperature fields. *Geophys. Res. Lett.,* **25,** 1297–1300.

——, and ——, 2000: Annular modes in the extratropical circulation. Part I: Month-to-month variability. *J. Climate,* **13,** 1000–1016.

——, and ——, 2001: Regional climate impacts of the Northern Hemisphere annular mode. *Science,* **293,** 85–89.

van Loon, H., and J. C. Rogers, 1978: The seesaw in winter temperatures between Greenland and northern Europe. Part I: General description. *Mon. Wea. Rev.,* **106,** 296–310.

Yoden, S., 1990: An illustrative model of seasonal and interannual variations of the stratospheric circulation. *J. Atmos. Sci.,* **47,** 1845–1853.

Walker, G. T., and E. W. Bliss, 1932: World Weather V. *Mem. Roy. Meteor. Soc.,* **4,** 53–83.

Woodruff, S. D., R. J. Slutz, R. L. Jenne, and P. M. Steurer, 1987: A comprehensive ocean–atmosphere data set. *Bull. Amer. Meteor. Soc.,* **68,** 1239–1250.